Volume 3 no.3 March 1976 Nucleic Acids Research

# Conformation and reactivity of DNA in the complex with proteins. III. Helix-coil transition and conformational studies of model complexes of DNA's with poly-L-histidine$^{+}$.

G.Burckhardt, Ch.Zimmer and G.Luck.

Akad. der Wissenschaften der DDR, Forschungszentrum für Molekularbiol. und Med., Zentralinst. für Mikrobiol. und exp. Ther., Abt. Biochem., DDR-69 Jena, Beuthenbergstr. 11, GDR

Received 8 December 1975

## ABSTRACT

Differences in the interaction of poly-L-histidine with DNA of various base composition have been demonstrated using melting and CD measurements. The two types of complexes formed with DNA at pH values below the pK of 5.9 and in the region of pH 6.5 are very different in their CD spectral properties. The binding effects with highly protonated poly-L-histidine are AT-dependent as reflected by large negative CD spectra indicating the formation of Ψ-DNA as a condensed state of the double helix. GC-rich DNA may, however, also form Ψ-DNA structures with poly-L-histidine under certain conditions. At pH 6.5 complex formation with the weakly protonated polypeptide is GC-dependent. From the results it is concluded that protonated poly-L-histidine interacts more specifically at AT base pairs, probably along the small groove while the weakly protonated poly-L-histidine tends to interact preferentially with GC regions which seems to occur rather in the large groove.

## INTRODUCTION

The genetic activity of eukaryotes is closely related to the interactions between DNA and proteins in chromatin (1,2). Studies on the binding effects of various synthetic polypeptides provide evidence for the possible role of individual amino acid residues in the complex formation with DNA (3-16). As widely occuring residues in histones the basic amino acids lysine and arginine have been intensively investigated in their polypeptide complexes with DNA (3-16). Recently, DNA complexes of polypeptides of defined sequence containing lysine, alanine and proline were described (14,17). There is, however, little known about the effects of nonbasic and minor amino acids in the polypeptide interaction. The possible importance of aromatic amino acid residues in the protein-DNA recognition interaction has been inferred in studies of Helene

et al. (19-21) and was further examined by other investigators using oligopeptides containing tyrosine, tryptophane or phenylalanine (22-25). Binding of poly-L-tyrosine and poly(L-lysine, L-tyrosine) to DNA was demonstrated in recent reports (26,27). Similar data have not yet published for histidine containing polypeptides. Since histidine is contained in histones, in chromosomal nonhistone proteins as well as in several enzymes we directed our attention to the interaction of poly-L-histidine with DNA (28-30). Histidine dissociates within the physiological pH region and may therefore affect the binding properties of a discrete oligopeptide segment.

In the present comprehensive study new data on the melting behaviour and CD spectral properties of polyhistidine complexes with various DNA's will be reported in order to evaluate the conformational effects associated with this complex formation. Two different types of DNA conformations apparently exist in the complex, the formation of which depends on GC content, salt concentration and on the pH of the solution. Chemical methylation is shown to affect the formation of the chirooptical active aggregates. The results suggest a preferential affinity of highly protonated polyhistidine as a random coil to AT base pair regions and a higher binding tendency to GC segments when it adopts an ordered form.

## EXPERIMENTAL

Poly-L-histidine with a molecular weight of 6.200 was obtained from Miles Laboratories Elkhard/Indiana. DNA from bacterial sources and calf thymus were that as previously described (31, 32): Streptomyces chrysomallus, 72 mole-% G+C, $\varepsilon$(P) = 6200; Sarcina maxima, 29 mole-% G+C, $\varepsilon$(P) = 6500; calf thymus, 42 mole-% G+C, $\varepsilon$(P) = 6600; Proteus mirabilis, 42 mole-% G+C, $\varepsilon$(P) = 6500; Escherichia coli B, 53 mole-% G+C, $\varepsilon$(P) = 6800. DNA, chemically methylated at N-7 of guanine sites was described elsewhere (33).

Ultraviolet absorbance measurements and melting experiments were carried out in a Uvispec spectrophotometer of Hilger & Watts, London, Ltd. $dh_{260}$ (T)/dT is the derivative of melting curve. Solutions were adjusted or titrated to the desired pH before the measurements using a pH-meter, model pH M-4 of

Radiometer, Copenhagen. CD spectra were recorded with a Cary 60 spectropolarimeter equipped with 6001 CD attachment. The specific ellipticity $[\Psi]$ was calculated on the basis of $E^{1\%}_{1cm}$ values as previously given (34). $[\Psi]$ is expressed in units of degrees·ml·$dm^{-1}$·$g^{-1}$ and the residual molar ellipticity $[\theta]$ in degrees·$cm^2$·$dm^{-1}$. DNA concentrations were in the range $10^{-4}$ to $1.5 \cdot 10^{-4}$ M.

Preparation of poly-L-histidine complexes: Annealed complexes were prepared by salt-gradient dialysis similar to the procedure of Huang et al. (35) with some modifications. Dialysis at constant pH, method A: At the initial salt concentration of 2 M, components were mixed at pH below the pK; dialysis steps at 4° C, three hours each, were: 0.4 M, 0.3 M, 0.15 M NaCl containing $10^{-3}$ M EDTA, then several times against final concentration. The pH was carefully controlled for all dialysis steps. Solvents were all unbuffered and the pH adjusted by addition of HCl or alkali. The initial pH at 2 M NaCl was maintained at pH 5 or pH 5.2 during all dialysis steps. This step is important for efficient complex formation of the protonated form of polyhistidine (see CD results). Dialysis with pH gradient, method B: A second procedure involves a pH gradient corresponding to the salt steps (0.4 M - pH 3.9; 0.3 M - pH 4.3; 0.15 M - pH 4.7; 0.1 M - pH 5.0 - pH 5.2). No appreciable loss of the polypeptide could be measured during the whole procedure. Concentrations reported are calculated as input ratios, r, based on defined histidine content of the polypeptide solution and on $\varepsilon$(P) values of DNA's. DNA solutions free from polypeptide were used in a parallel run for comparison. Occasionally occuring complexes with some precipitation were not used.

## RESULTS AND DISCUSSION

Helix-coil transitions: As previously demonstrated (28) poly-L-histidine changes its binding properties to DNA in the pH-range where the imidazolic residues of the polymer dissociate (36-42). The protonated imidazolic groups in the side chain of the polymer shown in Fig. 1 are the essential sites responsible for the variation of the binding effects observed in the denaturation profiles and CD of the complexes with DNA. In addition the coil to ordered conformational transition (40,

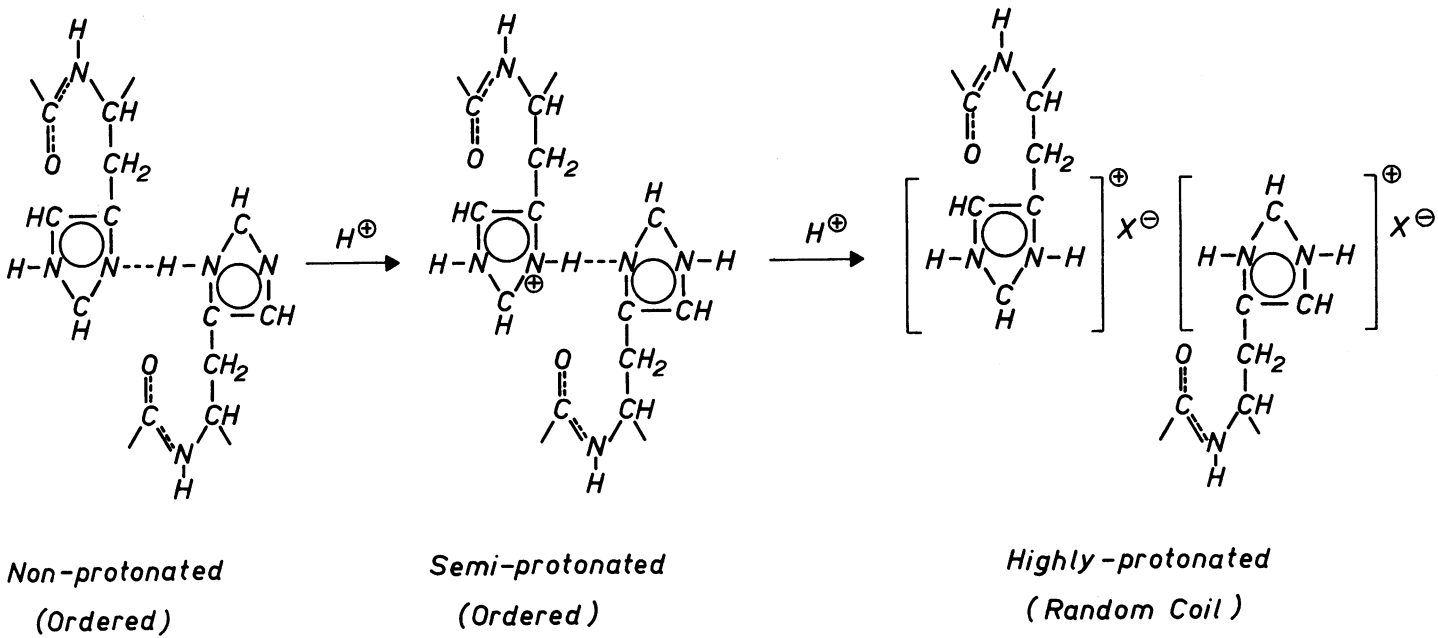


Fig. 1 Schematic drawing of protonation and possible hydrogen bonds between imidazole residues of poly-L-histidine according to Zundel and Muehlinghaus (49).

41) may also affect the interaction with DNA (see CD results). Binding of the highly protonated random coil of poly-L-histidine (38-42) to DNA at lower pH is demonstrated by typical melting profiles and their derivative curves as shown in Figs. 2 and 3 for DNA from calf thymus and very GC-rich DNA from Streptomyces chrysomallus. A biphasic melting is observed at pH 6.3 to 6.5 and at pH 5.1 of the calf thymus DNA in the presence of increasing r' ratios. Complex formation is indicated by the second melting step whereas the first transition represents melting of free DNA. The biphasic melting shows more typical differences in the case of the salt annealing procedure (method A) than those found in simple mixing experiments (not shown). The larger increase of the second transition towards higher temperature, the decrease of the hyperchromicity and an increased cooperativity in the second melting transition are characteristic for the differences in the binding between highly and weakly protonated poly-L-histidine to DNA at pH 5.1 and pH 6.5, resp. (Fig. 2). The first derivative melting curves more clearly demonstrate the complex formation between DNA and the protonated polypeptide. Very similar melting behavior was observed in complexes with DNA of 29 mole-% GC content. In the case of GC-rich DNA (72 mole-%), however, the first transition of free DNA is less influenced (derivative curves Figs. 3d and 4b) and precipitation occured at higher temperatures so that no second transition could be measured (Fig. 3). This may be due to enhanced interstrand cross-linking and decreasing solubility of the protonated GC-rich DNA when bound to poly-L-histidine at acidic pH. Apparently GC-rich DNA is less affected on interaction with protonated poly-L-histidine under these conditions.

Measurements of absorbance changes above 300 nm due to light scattering during melting were followed in almost all cases. As an example Fig. 4 demonstrates that an increased scattering contribution to the absorbance at 340 nm is involved in the second melting transition, i.e. when melting of the DNA complex occurs. The UV-absorption spectra of the DNA-polypeptide complexes in the pH region below pH 6 exhibit light scattering effects above 300 nm with increasing r' ratio

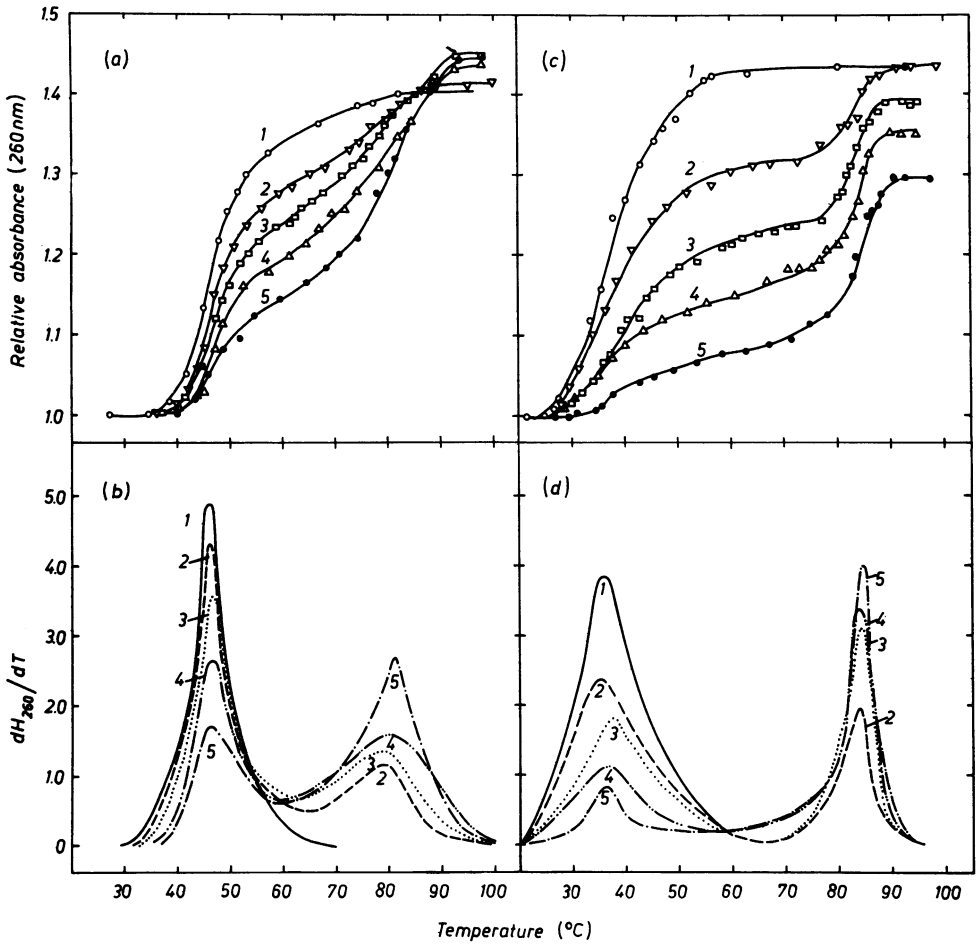


Fig. 2 Melting profiles of calf thymus DNA - poly-L-histidine complexes prepared by salt gradient dialysis, method A; buffer see Fig. 1. Numbers denote input ratio, r: histidine DNA-P as follows: (a) pH 6.3, r' = 0, 0.3, 0.5, 0.7, 1.0 correspond to curves 1, 2, 3, 4 and 5; (c) pH 5.1, r' = 0, 0.3, 0.5, 0.7, 0.9 correspond to curves 1, 2, 3, 4 and 5; (b) and (d) are the derivative curves of the hyperchromicity (given by relative absorbance) with respect to temperature, numbers correspond to r' of (a) and (c) respectively.

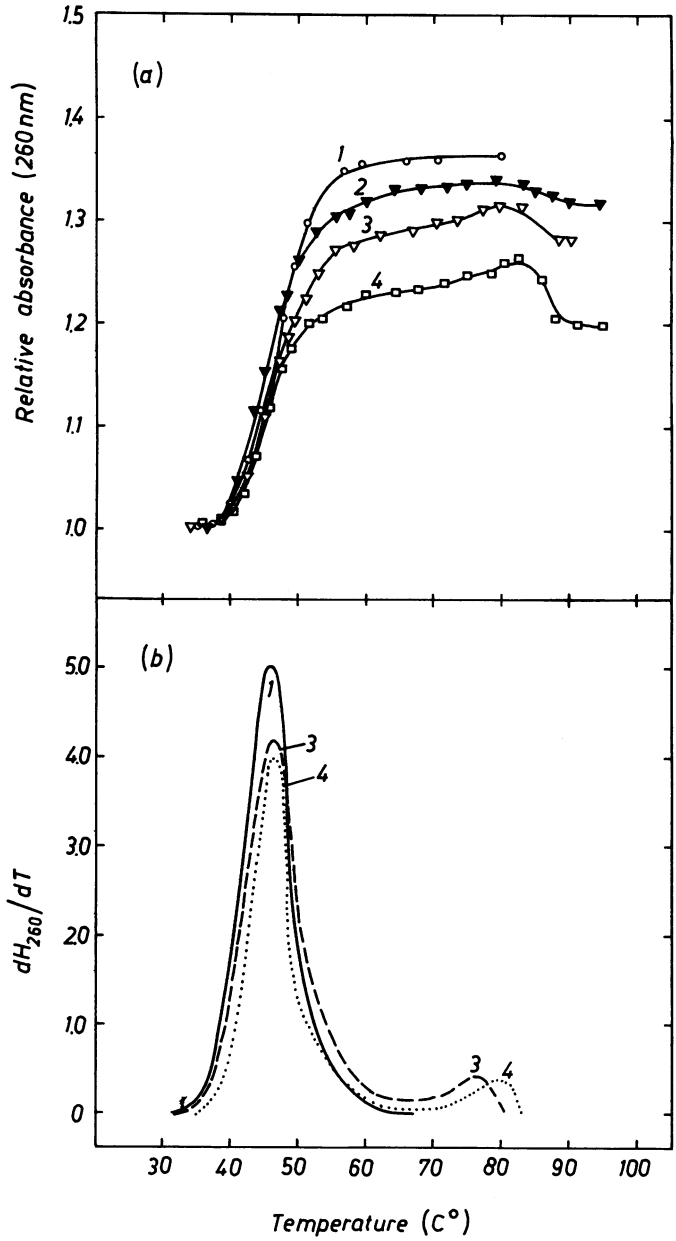


Fig. 3 Melting profiles of DNA-poly-L-histidine complexes from Streptomyces chrysomallus (72 mole-% G+C) prepared by salt gradient dialysis; pH 5, buffer see Fig. 1. (a) Numbers denote input ratio r' histidine/DNA-P as follows: r' = 0, 0.1, 0.3, 0.5 correspond to curves 1, 2, 3 and 4. (b) Derivative curves of the hyperchromicity with respect to temperature, numbers correspond to that in (a).

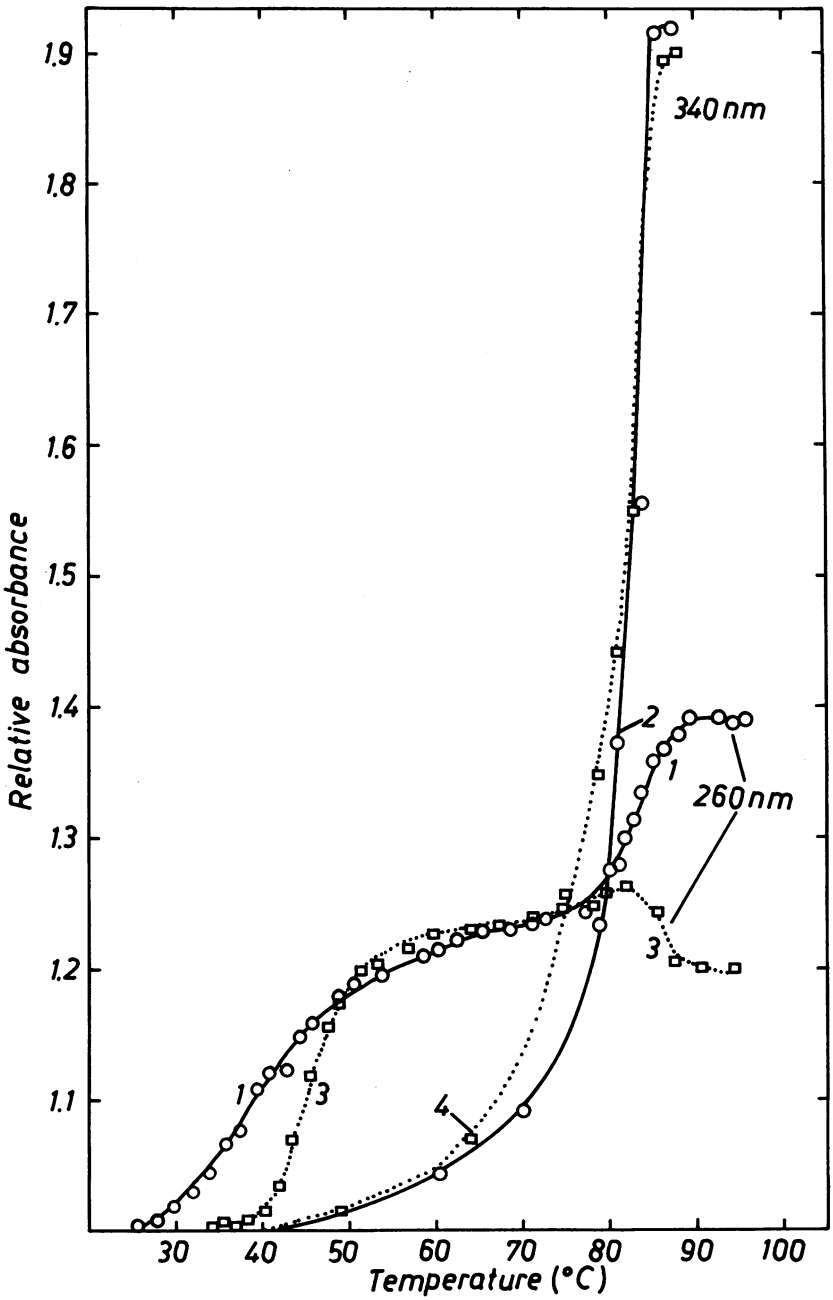


Fig. 4 Comparison of the melting of the DNA-poly-L-histidine complex monitored at 260 nm and 340 nm, buffer see Fig. 1; Sarcina maxima at pH 5.5 curves 1 and 2, Streptomyces chrysomallus at pH 5.1 curves 3 and 4.

histidine to nucleotide. The influence around 260 nm was not very large. This could be explained by opposite signs resulting from a hypochromic change around 260 nm on formation of the condensed state and a scattering contribution. In the region pH 6.3 or higher the light scattering increase was less than 25 % from that of the complexes with highly protonated poly-L-histidine (29).

The melting data (Fig. 2) suggests that AT-rich regions seem to favour the complex formation with the highly protonated form of poly-L-histidine. In the following report we will demonstrate, that GC-rich DNA also generates the $\psi$-state due to binding poly-L-histidine at high ionic strength, but the $\psi$-type binding effect is primarily achieved by AT pairs. In analyzing the melting data of Fig. 2 the fraction of base pairs covered by histidine residues can be estimated using the following equation according to Li et al. (43,44):

$$R' = ß \left(1 - \frac{A_f}{h_f}\right)$$

where R' represents the input ratio of histidine residue per nucleotide, ß is the number of histidines per nucleotide in covered regions, $A_f$ is the melting area at $T_m$ of the first transition (derivative curve) and $h_f$ defines the hyperchromicity of free DNA fractions. The linear plot shown in Fig. 5 yields ß = 1.0 for polyhistidine at pH 5.2. This suggests that 1 histidine residue per 1 nucleotide cause the complete complexing on binding to highly protonated polyhistidine, which means that 1 protonated histidine unit is bound to 1 nucleotide. The charged polyhistidine coil behaves similar as poly-L-lysine and poly-L-arginine (3,5) in neutralizing negative sites along DNA. At pH 6.3 a mean value of ß $\sim$ 1.7 is obtained from Fig. 7 which can be interpreted by a larger fraction of histidine residues per nucleotide in covered regions necessary to produce stabilization and efficient complex formation. This would mean that the interaction of the histidines of the polypeptide is less efficient probably due to the deprotonated ordered polyhistidine structure (41, 42). This preferential affinity of histidine residues at

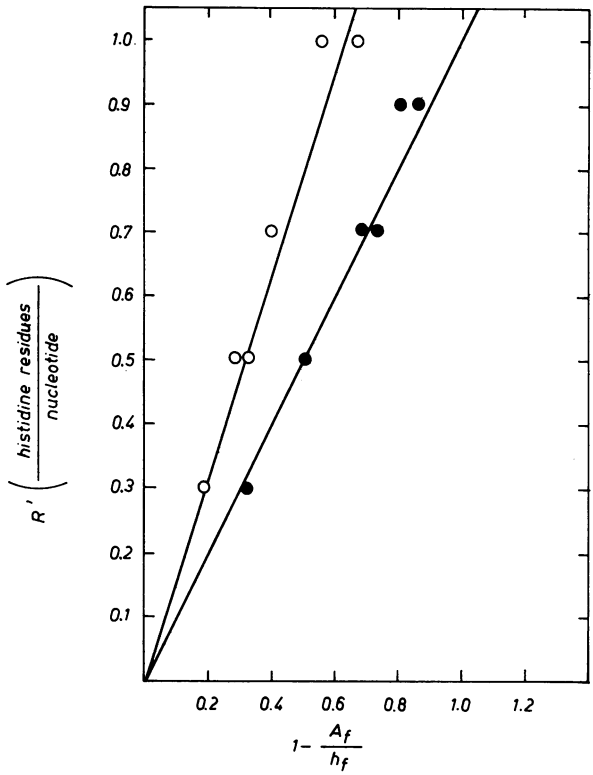


Fig. 5 Binding of poly-L-histidine to calf thymus DNA at pH 5.2 (●) and pH 6.5 (o).

acidic pH to AT-rich sites of DNA is similar as reported for poly-L-lysine binding to AT-rich regions in DNA (4,45,46). The following CD results strongly supports the melting data.

Circular Dichroism: In a previous work (28) we have shown that complex formation of DNA with protonated poly-L-histidine is associated with the appearance of large negative CD amplitudes characteristic of a $\Psi$ -type CD spectrum (30,47,48). The effectiveness of the formation of this $\Psi$-type DNA depends on the pH conditions during dialysis steps as demonstrated by a reinvestigation using method B. Fig. 6 shows very large negative CD amplitudes when dialysis starts from pH 3.9 at 0.4 M NaCl and increases continuously to pH 5 on decreasing the salt molarity to 0.1 M. It must be mentioned that the

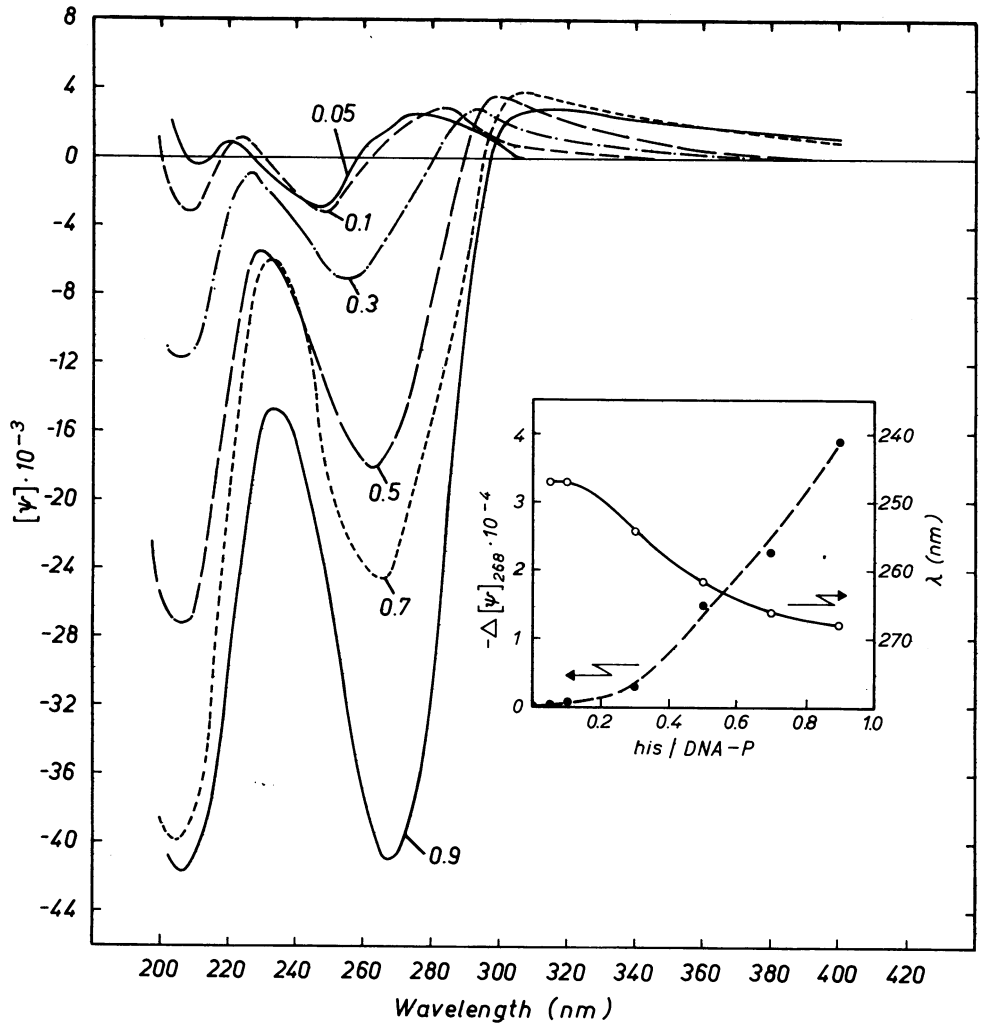


Fig. 6 Binding of protonated poly-L-histidine to calf thymus DNA as reflected by their CD spectra at 0.1 M NaCl. Complexes prepared by method B using dialysis with salt and pH gradient: 0.4 M, pH 3.9; 0.3 M, pH4.3; 0.15 M, pH 4.7; 0.1 M NaCl, pH 5.0. Attached numbers indicate increasing ratio r'.

degree of protonation of GC pairs decreases with increasing salt molarity and the pH's selected in the different salt steps are at 4° and 25°C far from the onset of denaturation (52). According to a previous estimation of protonated cyto-

sine residues in DNA some rough values may characterize this point: e.g. at 0.02 M NaCl around pH 4 less than 30 % and at pH 5 about 5 to 10 % of G-C pairs should be protonated in DNA (52). These values are further lowered at 0.4 M and 0.1 M so that under final conditions (pH 5 to pH 5.2) the relative amount of protonated base pairs to all pairs is negligible for calf thymus DNA. The anomalous CD spectrum around 265 nm demonstrates the formation of the $\Psi$-DNA structure with increasing r', histidine/DNA-P, indicating a linear ascending part beyond r' of 0.4 (insert of Fig. 6). Complex formation at constant pH according to method A results in about seven to ten times lower negative CD amplitudes (not shown). The most likely explanation is, that the ordered secondary structure of poly-L-histidine dependent on the degree of protonation (38-42,49,50) influences the formation of the condensed $\Psi$-state of DNA. In the region of semiprotonation histidine residues are linked by a shared proton between two imidazole rings (Fig. 1) forming an ordered structure (38-42) and thus the binding to DNA is less effective. This picture may qualitatively describe the state in method A. At lower pH (Fig. 1) the more strongly protonated histidines in the polymer will repel each other so that the favoured random coil form (38-42,50) may interact most efficiently with the negative sites along the DNA double helix which is achieved in steps of method B. The $\Psi$-type CD spectrum of the highly protonated coil form of polyhistidine is similar as previously reported for polylysine (8). As demonstrated by various authors the $\Psi$-type CD spectrum is the result of some kind of aggregation or any other ordered compact structure (8,14,17,30,47,48,51). Light scattering changes (Table 1) at 340 nm together with high speed centrifugation demonstrate that aggregates are involved in the DNA complexes with highly protonated polyhistidine. After centrifugation at 10000 x g a large amount of the complex remains still in the supernatant while at 45000xg the polyhistidine complex is completely sedimented within 30 minutes. Weakly protonated polyhistidine forms a complex with DNA at pH 6.5 associated with a lower scattering contribution to the absorbance at 340 nm (Table 1). Comparison of the values

Table 1 Effect of high speed centrifugation on extinction at 260 and 340 nm of the DNA-poly-L-histidine complex from calf thymus at 0.1 M NaCl, prepared according to method B, r' = 0.7 histidine/DNA-P

| Centrifugal force | pH ~ 5 | | pH = 6.5 | |
|---|---|---|---|---|
| (g) | $E_{260}$ | $E_{340}$ | $E_{260}$ | $E_{340}$ |
| 0 | 0.794 | 0.158 | 0.800 | 0.044 |
| 10 000 | 0.197 | 0.020 | 0.325 | 0.030 |
| 45 000 | 0.082 | 0.005 | 0.200 | 0.005 |

in Table 1 suggest that a greater amount of the complex at pH 6.5 remains in the supernatant.

The CD change of the DNA complex with polyhistidine and that of the free polypeptide at different pH is shown in Fig. 7. A relatively sharp transition between the two types of CD spectra occurs in the pH region where free poly-L-histidine dissociates and the random coil conformation with high degree of protonation of the imidazolic groups undergoes a transition to an ordered polypeptide structure with lower degree of protonation (41,42). This may be an indication for different types of the interaction with the helical DNA structure. Association of the polyhistidine with DNA to form the $\Psi$-state is most efficient when the extended random coil with high degree of protonation of histidine side chains binds to the grooves (Figs. 2, 6). Fig. 7 indicates that deprotonation of poly-L-histidine between pH 7 and pH 8 again decreases the CD. The pKa' of poly-L-histidine depending on its secondary structure (40,41) may be further displaced due to the poly-anionic nature of the DNA but in view of the transition in the DNA complex between pH 6 and 6.5 and of the proton-dependent conformational change of free poly-L-histidine (Fig. 7) this pK-shift should not be greater than half a pH unit. To characterize the influence of base composition on the binding effects of the two states of DNA in the complex with poly-histidine typical different CD spectral properties of extremely AT-rich and GC-rich DNA are displayed in Figs. 8 and 9. All other data are summarized in Table 2. Extremely AT-rich DNA

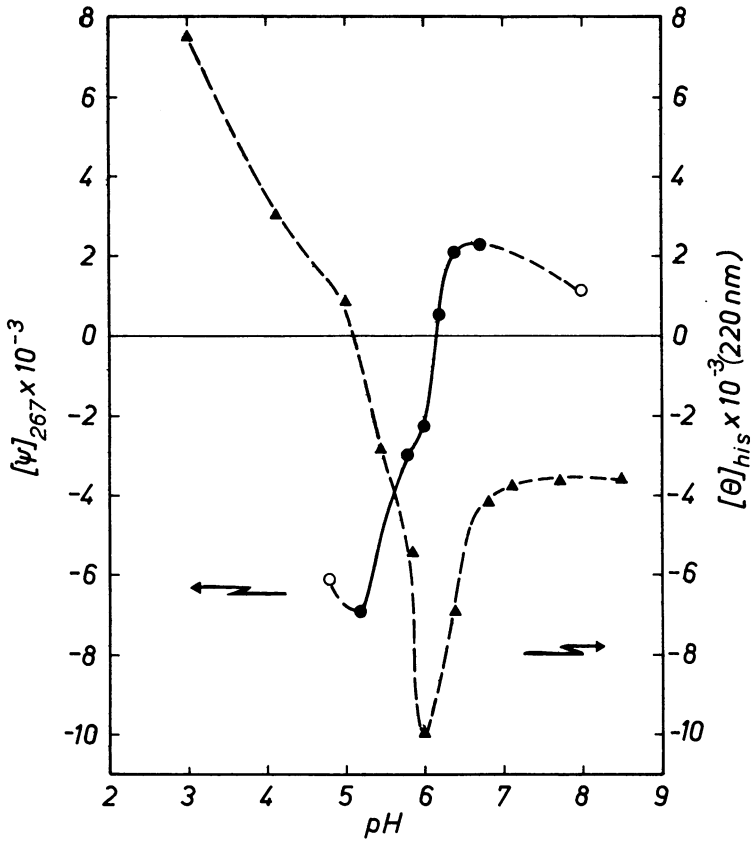


Fig. 7 Variation of CD at 267 nm of the calf thymus DNA-poly-L-histidine complex (o-o-o) and free poly-L-histidine at 220 nm ( -- -- ) with pH in 0.1 M NaCl.

from Sarcina maxima (Fig. 8) exhibits no anomalous negative CD amplitude on polyhistidine binding at pH 5.5, but a positive CD maximum is observed at 290 nm indicating interaction with the DNA. In the range of pH 6.5 to pH 7.5 binding is associated with a lowering of the positive CD maximum at 279 nm. In contrast to that GC-rich DNA shows a positive non-conservative spectrum at pH 6.5 with a large positive CD amplitude at 270 nm but no negative Ψ-type CD spectrum between pH 5.2 - 4.5 under these salt conditions (Fig. 8). Several DNA's examined support this principal different behaviour (Table 2). GC-rich DNA forms no Ψ-DNA state on

Table 2 CD data of poly-L-histidine complexes of DNA's from various sources in 0.1 M NaCl, prepared according to method A and B, at 0.7 histidine/DNA-P; a) at 0.6; b) at 0.5 histidine/DNA-P; c) in 2 M NaCl.

| DNA | A+T mole-% | Method of Dialysis | pH | $\lambda_{max_1}$ (nm) | $\Delta\varepsilon$ | $\lambda_{max_2}$ (nm) | $\Delta\varepsilon$ | pH | $\lambda_{max}$ (nm) | $\Delta\varepsilon$ |
|---|---|---|---|---|---|---|---|---|---|---|
| Streptomyces chrysomallus a) | 28 | A | 5.2 | 302 | -0.15 | 280 | 0.60 | 6.5 | 270 | 4.50 |
| Micrococcus lysodeikticus b) | 28 | A | 5.1 | 307 | -0.17 | 271 | 2.40 | 6.2 | 267 | 4.30 |
| Escherichia coli | 50 | A | 5.2 | none | - | 263 | -2.85 | 6.7 | 270 | 1.60 |
| calf thymus | 58 | A | 5.2 | 302 | 0.35 | 260 | -7.00 | 6.7 | 270 | 2.65 |
| Proteus mirabilis | 58 | A | 5.3 | 305 | 0.20 | 255-60 | -3.30 | 6.6 | 274 | 1.30 |
| Sarcina maxima | 71 | A | 5.5 | 293 | 1.25 | 250 | -4.10 | 6.5 | 279 | 1.80 |
| Poly(dA-dT)·(dA-dT) | 100 | A | 5.2 | 297 | 3.64 | 268 | -15.00 | 6.5 | 295 | 2.12 |
| Poly(dA)·(dT) | 100 | A | 5.2 | 293 | 10.30 | 265 | -18.30 | 6.8 | 289 | 2.42 |
| Streptomyces chrysomallus c) | 28 | A | 4.0 | none | - | 266 | -7.20 | 6.3 | 270 | 1.70 |
| Streptomyces chrysomallus | 28 | B | 5.1 | none | - | 260 | -2.0 | - | - | - |
| calf thymus | 58 | B | 5.1 | none | - | 269 | -35.5 | - | - | - |
| T2 phage | 39 | B | 5.1 | none | - | 270 | -15.7 | 6.4 | 278 | 1.2 |
| Sarcina maxima | 71 | B | 5.2 | 304 | 1.90 | 266 | -24.2 | - | - | - |
| Poly(dA-dT)·(dA-dT) | 100 | B | 5.1 | 355 | 0.45 | 273 | -113.0 | - | - | - |
| Poly(dA)·(dT) | 100 | B | 5.1 | 293 | 11.90 | 265 | -19.4 | - | - | - |

binding with highly protonated polyhistidine at 0.1 M NaCl (Fig. 9, Table 2). According to our results presented in the subsequent paper this restriction may be attributed to the presence of protonated GC-base pairs, and the $\psi$-type DNA is observed at very high salt concentration in this case. The formation of $\psi$-type CD spectra for AT-rich DNA complexes at 0.1 M NaCl using dialysis method B is displayed in Fig. 10. Results of various DNA's are summarized in Table 2. The large negative CD amplitudes in the region of 260 to 270 nm show an AT-dependent binding effect with highly protonated polyhistidine around pH 5.2 which is most efficient when method B is used. In addition to that the occurrence of the positive CD band between 293 and 305 nm is typical for AT-rich DNA polyhistidine complexes and resembles that found for DNA polymers containing 100 % dA·dT pairs (Table 2 and subsequent paper). These CD bands are accompanied by long-wavelength trails with positive ellipticities (Figs. 6 and 8). Since the trails occur in the nonabsorptive spectral region ($\lambda > 300$ nm) and our complexes exhibit light-scattering contribution to the absorbance beyond 300 nm their origin could be attributed

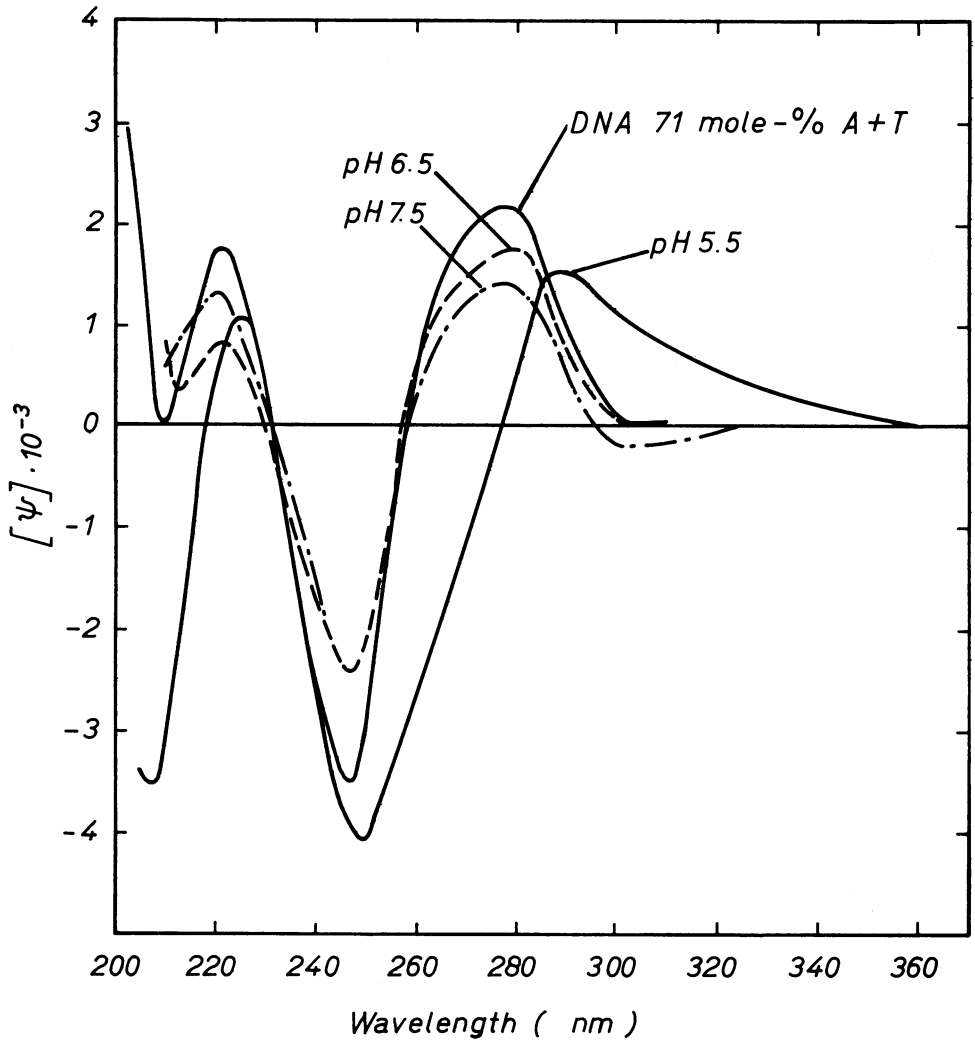


Fig. 8 Dependence of CD spectra of the AT-rich DNA-L-histidine complex on pH prepared by method A; at 0·1 M NaCl, r' = 0·6 histidine/DNA-P.

to scattering artifacts. We wish to emphasize, however, that some other factors should be also considered for the following reasons. Both, AT-rich and GC-rich DNA's exhibit scattering contribution around 340 nm with signs of similar order but they greatly differ in their CD spectral behaviour and in no case a positive CD band with large trail beyond 300 nm could

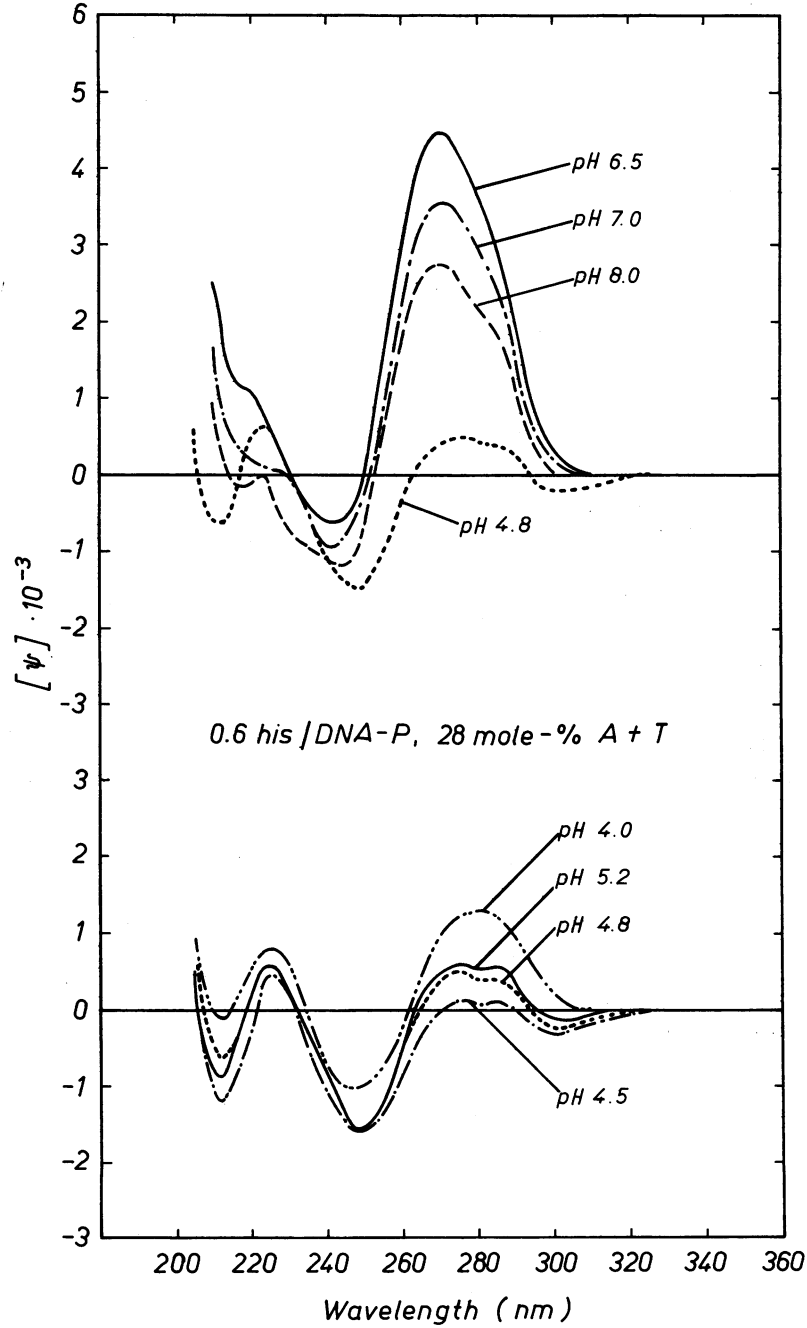


Fig. 9 Dependence of CD spectra of the GC-rich DNA-poly-L-histidine complex on pH prepared by method A; at 0.1 M NaCl, r' = 0.6 histidine/DNA-P.

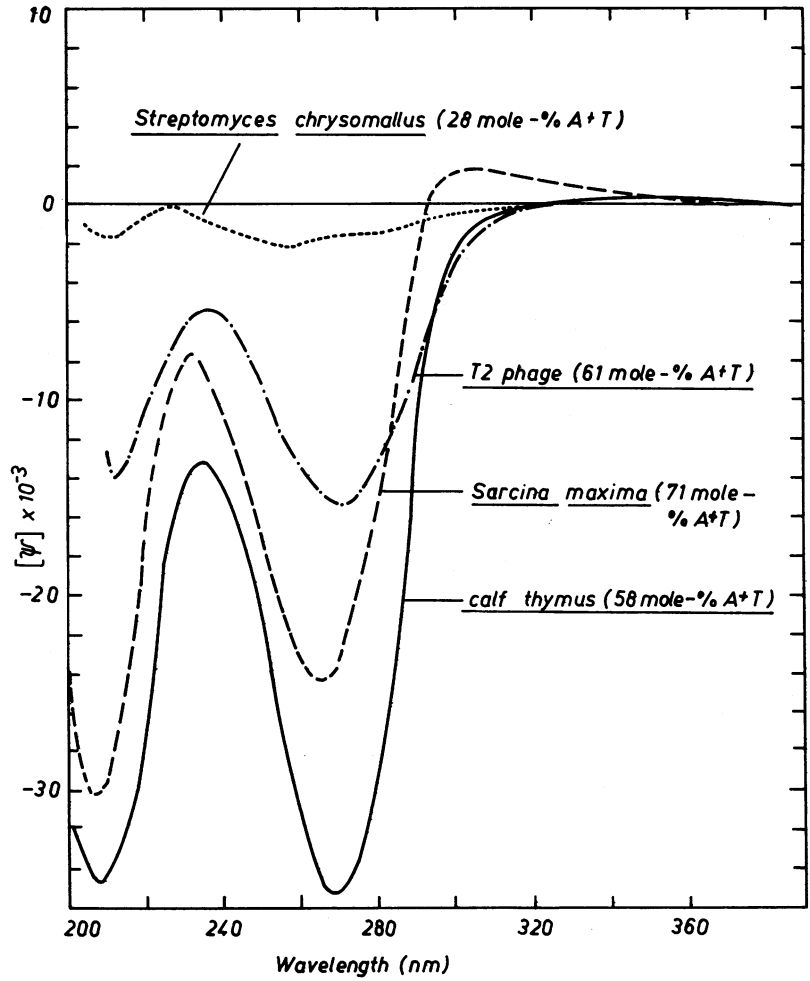


Fig. 10 - type CD spectra of poly-L-histidine complexes of various DNA's at 0.1 M NaCl prepared according to method B; r' = 0.7 histidine/DNA-P.

be observed for GC-rich DNA. As an example at r' = 0.6 to 0.7 histidine calf thymus DNA and Streptomyces chrysomallus DNA showed a maximal increase from $E_{340}$ = 0.005 to 0.20 and 0.19, resp. The former corresponds to a ψ-type CD spectrum with a band around 300 nm similar as shown in Fig. 6 while no anomalous CD band with a positive long wavelength band appears for Streptomyces chrysomallus DNA (Fig. 9, pH 4 to pH 5.2).

Recent findings also indicate very high sedimentation coefficients of the same order for both DNA complexes albeit completely different CD spectra (53) were observed.

This suggests that light-scattering aggregates of the complexes not necessarily generate positive long-wavelength trails and $\Psi$-type CD spectra. In the recent work of Cheng and Mohr (54,55) it was stressed on the evidence of scatter-corrected CD spectra of $\Psi$-DNA in poly(ethylene oxide) that their spectra exhibit similar long-wavelength trails and hence cannot be simply attributed to scattering artifacts. They envisage these effects as contributions from the liquid crystalline structure of $\Psi$-DNA, which is supported by CD results of the T2 phage (56). The superstructure of $\Psi$-DNA in the protonated polyhistidine complex may represent a similar ordered structure of liquid crystalline nature. The dependence on AT-content of the long-wavelength trail may originate from binding effects to AT pairs, the importance of which will be discussed in a second paper (57).

Around pH 6.5 (Table 2) greater $\Delta\varepsilon$ values of the complexes and spectral shifts (Fig. 9) appear for GC-rich DNA's indicating a preferential interaction of the ordered poly-L-histidine structure at low degree of protonation with (dG·dC)-rich regions.

CD binding effects of methylated DNA: Since selective methylation of N-7 of guanine affects the conformation of GC base pair regions as well as binding in the large groove of the helix, methylated DNA provides some valuable information for the mechanism of interaction with the polypeptide. CD results of poly-L-histidine complexes formed with DNA of increasing degree of methylated guanine residues are shown in Fig. 11. As indicated by the $\Psi$-type CD spectrum the complex formation at pH 5.1 is reduced, but still maintained at 20 % methylation and disappears at 40 % methylation. At pH 6.5 20 % methylated guanines cause already complete disappearance of the characteristic positive non-conservative spectrum (Fig. 11) indicating a higher sensitivity of this complex to methylation. As expected the GC-rich DNA complex was found to be also extremely sensitive to the guanine specific methylation at pH 6.5 (not shown).

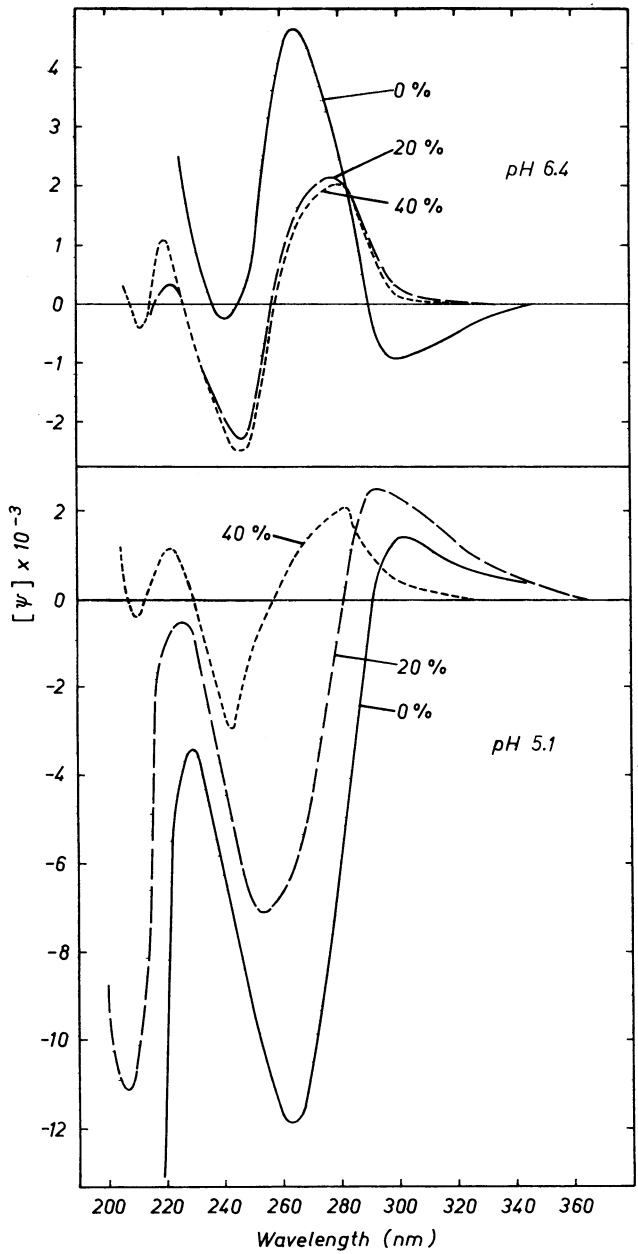


Fig. 11 Effect of methylation on the calf thymus DNA-poly-L-histidine complex at 0.1 M NaCl, pH 5.1 and pH 6.4, 0.5 histidine/DNA-P.

The results suggest the importance of GC base pairs for the efficient binding of the ordered polyhistidine at pH 6.5 and their contribution to the formation of the Ψ-state of DNA at lower pH. This agrees with the conclusions (55,58) that the superstructure formation of the Ψ-state depends on GC-content. Recent findings on Ψ-DNA complexes with histones and f1 likewise demonstrate a depression of Ψ-type structures of methylated GC-rich DNA (59). The specific methylation of guanine in DNA reduces the accessibility of the large groove and induce a conformational change with decreasing tendency in helical twisting (60) and hence, the binding effects of polyhistidine are diminished. This may be an indication that at pH 6.5 the interaction of polyhistidine involves the large groove of the helix.

## CONCLUSIONS

The present data show that two types of complexes are formed between poly-L-histidine and DNA by modulating the binding properties and conformation of the polypeptide due to changes in the degree of protonation of histidine residues. A Ψ-type DNA of ordered condensed structure is indicated when poly-L-histidine exists in the highly protonated state and the polymer has coil conformation. For this type of interaction an AT affinity of protonated histidine groups predominates. The protonated or weakly protonated ordered form of the poly-L-histidine formed around pH 6.5, tends to interact mainly along GC-rich DNA regions. Our data suggest that the specificity of the interacting groups of polyhistidine with DNA depends on conformation of the polypeptide and DNA.

Acknowledgement: We thank Dr. H. Triebel for his great interest and helpful comments.

+ Publication no. II in this series see ref. 28

## REFERENCES

1 Hearst, J. and Botchan, M. (1970) Ann. Rev. Biochem. 39, 151-182
2 DeLange, R. J. and Smith, E. L. (1971) Ann. Rev. Biochem. 40, 279

3 Tsuboi, M., Matsuo, K. and Ts'o, P. O. P. (1966)
J. Mol. Biol. 15, 256-267
4 Leng, M. and Felsenfeld, G. (1966)
Proc. Natl. Acad. Sci. (US) 56, 1325-1333
5 Olins, D. E., Olins, A. L. and von Hippel, P. H. (1967)
J. Mol. Biol. 24, 157-176
6 Kawashima, S., Inoue, S. and Ando, T. (1969)
Biochim. Biophys. Acta 186, 145-157
7 Shih, T. Y. and Bonner, J. (1970)
J. Mol. Biol. 48, 469-487
8 Zama, M. and Ichimura, S. (1971)
Biochem. Biophys. Res. Commun. 44, 936-942
9 Carroll, D. (1972) Biochemistry 11, 421-426
10 Chang, C., Weiskopf, M. and Li, H. J. (1973)
Biochemistry 12, 3028-3032
11 Li, H. J., Chang, C. and Weiskopf, M. (1973)
Biochemistry 12, 1763-1772
12 Li, H. J., Brand, B. and Rotter, A. (1974)
Nucleic Acids Res. 1, 257-265
13 Li, H. J., Chang, C., Weiskopf, M., Brand, B. and Rotter,
A. (1974) Biopolymers 13, 649-667
14 Sponar, J., Stokrova, S., Koruna, I. and Blaha, K.(1974)
Collection Czechoslov. Chem. Commun. 39, 1625-1645
15 Zama, M. and Ichimura, S. (1973)
Biochim. Biophys. Acta 294, 214-226
16 Zama, M. (1974) Biochim. Biophys. Acta 366, 124-134
17 Sponar, J., Fric, I. and Blaha, K. (1975)
Biophys. Chem. 3, 255-260
18 Helene, C., Dimicoli, J.-L. and Brun, F. (1971)
Biochemistry 10, 3802-3809
19 Helene, C. (1971) Nature New Biol. 234, 120-121
20 Dimicoli, J. L. and Helene, C. (1974)
Biochemistry 13, 714-723
21 Dimicoli, J. L. and Helene, C. (1974)
Biochemistry 13, 724-730
22 Novak, R. L. and Dohnal, J. (1973)
Nature New Biol. 243, 155-157
23 Novak, R. L. and Dohnal, J. (1974)
Nucleic Acid Res. 1, 753-759
24 Gabbay, E. J., Sanford, K. and Baxter, C. S. (1972)
Biochemistry 11, 3429-3435
25 Adawadkar, P., Wilson, W. D., Brey, W. and Gabbay, E. J.
(1975) J. Amer. Chem. Soc. 97, 1959-1961
26 Friedman, S. and Ts'o, P. O. P. (1971)
Biochemistry 10, 3099-3104
27 Santella, R. M. and Li, H. J. (1974)
Biopolymers 13, 1909-1926
28 Burckhardt, G., Zimmer, Ch. and Luck, G. (1973)
FEBS Letters 30, 35-39
29 Burckhardt, G. and Zimmer, Ch. (1973)
studia biophysica 38, 223-228
30 Zimmer, Ch., Burckhardt, G. and Luck, G. (1973)
studia biophysica 40, 57-62
31 Sarfert, E. and Venner, H. (1960)
Hoppe-Seyler's Z. Physiol. Chem. 340, 153-160
32 Sarfert, E. and Venner, H. (1962)
Naturwissenschaften 49, 423

33 Bauer, E., Berg, H., Löber, G., Weller, K., Hartmann, M. and Zimmer, Ch. (1974) Biophys. Chem. 1, 338-348
34 Zimmer, Ch., Luck, G., Thrum, H. and Pitra, Ch. (1972) Eur. J. Biochem. 26, 81-89
35 Huang, R. C., Bonner, J., Murray, K. (1964) J. Mol. Biol. 8, 54-64
36 Norland, K. S., Fassman, G. D., Katchalski, E. and Blout, E. R. (1963) Biopolymers 1, 277-278
37 Fasman, G. D. (1967) in "Poly-α-Amino Acids" (ed. G. D. Fasman), M. Dekker Inc., New York, Vol. 1
38 Patchornik, A., Berger, A. and Katchalski, E. (1957) J. Amer. Chem. Soc. 79, 5227-5228
39 Beychok, S., Pflumm, M. N. and Lehmann, J. E. (1965) J. Amer. Chem. Soc. 87, 3990-3991
40 Miyazawa, T. (1967) in "Poly-α-Amino Acids" (ed. G. D. Fasman), M. Dekker Inc., New York, Vol. 1
41 Myer, F. and Barnard, D. (1971) Arch. Biochem. Biophys. 143, 116-119
42 Terbojevich, M., Cosani, A., Peggion, E., Quadrifoglio, F. and Crescenzi, V. (1972) Macromolecules 5, 622
43 Li, H. J. (1973) Biopolymers 12, 287-296
44 Yu, S. S. and Li, H. J. (1973) Biopolymers 12, 2777-2788
45 Shapiro, J. T., Leng, M. and Felsenfeld, G. (1969) Biochemistry 8, 3219-3225
46 Ohba, Y. (1966) Biochim. Biophys. Acta 123, 84-87
47 Jordan, C. F., Lerman, L. S. and Venable, J. H. (1972) Nature New Biol. 236, 67-70
48 Evdokimov, Yu. M., Platonov, A. L., Tikhonenko, A. S. and Varshavsky, Ya. M. (1972) FEBS Letters 23, 180-184
49 Zundel, G. and Muehlinghaus, J. (1971) Z. Naturforschung 26 b, 546-555
50 Muehlinghaus, J. and Zundel, G. (1971) Biopolymers 10, 711-719
51 Brunner, W. C. and Maestre, M. F. (1974) Biopolymers 13, 345-358
52 Zimmer, Ch. and Venner, H. (1966) Biopolymers 4, 1073-1079
53 Burckhardt, G., Triebel, H., Zimmer, Ch., unpublished results
54 Cheng, S.-M. and Mohr, S. C. (1974) FEBS Letters 49, 37-42
55 Cheng, S.-M. and Mohr, S. C. (1975) Biopolymers 14,663-674
56 Holzwarth, G., Gordon, D. G., McGinness, J. E., Dorman, B. P. and Maestre, M. F. (1974) Biochemistry 13, 126-132
57 Burckhardt, G., Zimmer, Ch. and Luck, G., this journal
58 Sponar, J. and Fric, I. (1972) Biopolymers 11, 2317-2330
59 Sponar, J., Doskocil, J., Blaha, K. and Zimmer, Ch., to be published
60 Bauer, E., Berg, H., Löber, G., Weller, K., Hartmann, M. and Zimmer, Ch. (1974) Biophys. Chem. 1, 338-348